# SUPPLEMENTAL INFORMATION

## SUPPLEMENTAL FIGURE LEGEND

**Figure S1. A)** Representative images of control sections of paraffin-embedded LM2-GFP and LM2-mCherry cells grown separately (left) or as co-culture (right) and stained with anti-GFP (brown) and anti-mCherry (red) antibodies. **B)** Representative images of a LM2-GFP, a LM2-mCherry and a LM2-GFP/LM2-mCherry (1:1) primary tumor stained with antibodies anti-GFP (brown) and anti-mCherry (red). The LM2-GFP and LM2-mCherry tumors were present in the same animals. Arrows indicate mCherry-positive cells in the LM2-GFP tumor and GFP-positive cells in the LM2-mCherry tumor, respectively, as examples of tumor self-seeding. Related to Figure 1.

**Figure S2. A)** Table showing counts of one color versus multicolor events within CTCs and lung foci from both the "LM2-GFP/LM2-mCherry 1:1" and the "LM2-GFP (right) and LM2-mCherry (left)" models. Results represent means ± SEM. **B)** Distribution curve describing the expected numbers of GFP- or mCherry-only CTC-clusters per mouse given our experimental setup, with the actual value shown as a red dashed line (top). Representative pictures of LM2-GFP-only and mCherry-only CTC-clusters captured on the $^{HB}$CTC-chip from the blood of mice belonging to the "LM2-GFP/LM2-mCherry 1:1" model (bottom). Blood samples were isolated five weeks after primary tumor development. **C)** Table showing counts of one color versus multicolor events within CTCs and lung foci from both the "4T1-GFP/4T1-mCherry 1:1" and the "4T1-GFP (right) and 4T1-mCherry (left)" models. Mice were sacrificed for CTCs and lungs isolation three weeks after primary tumor development. Results represent means ± SEM (n=4) (left). Representative images of one color and multicolor 4T1 CTCs and lung foci (right). **D)** Bar graph showing the normalized metastatic potential of 4T1 single CTCs and CTC-clusters. n=4, *p<0.036 by Student's t test. Related to Figure 1.

**Figure S3. A)** Schematic showing BT474- or 4T1-GFP-Luciferase cells prepared as single cells (SC) or as clusters (CL) prior to injection into the tail vein of immunodeficient mice. **B)** Representative images of GFP-stained sections of mouse lungs after injection with BT474 or 4T1 SC versus CL (left). The bar graphs show the mean percentage of GFP-positive cells in lungs from mice injected with BT474 or 4T1 SC versus CL (right). n=4; NS= not significant, *p=0.003 **p=0.002 by Student's t test. **C)** Representative pictures of cleaved caspase 3-stained sections of mouse lungs 24 hours after injection with BT474 or 4T1 SC versus CL. The bar graph shows the mean percentage of cleaved caspase 3-positive cells in lungs from mice injected with BT474 or 4T1 SC versus CL. n=4; *p=0.037 **p=0.028 by Student's t test. **D)** Lung metastasis growth curves from mice injected with BT474 or 4T1 SC versus CL. n=4; ***p<0.02 *p<0.027 *p<0.05 by Student's t test. Related to Figure 2.

**Figure S4.** Heatmap showing expression levels of CTCs-, leukocytes-, T cells-, B cells-, dendritic cells-, natural killer (NK) cells-, hematopoietic stem cells-, macrophages/monocytes-, granulocytes-, platelets-, endothelial cells- and fibroblasts-associated transcripts in the 15 single CTCs and 14 CTC-clusters samples used to derive CTC-clusters upregulated transcripts. Related to Figure 5.

**Figure S5.** Kaplan-Meier distant metastasis-free survival plots showing progression rates for patients whose primary tumor expressed either "low" or "high" levels of the top CTC-clusters-associated marker genes. Related to Figure 6.

**Figure S6. A)** Heatmap showing expression levels of desmosomes (top) and adherence junctions (bottom) marker genes in the 15 single CTCs and 14 CTC-clusters samples used to derive CTC-clusters upregulated transcripts. **B)** Heatmap representing fold change of desmosomes (top) and adherence junctions (bottom) marker genes in all "CTC-clusters vs single CTCs" intrapatient comparisons. **C)** Heatmap showing fold change of desmosome (D) and adherence junction (AJ) metagenes in all "CTC-clusters vs single CTCs" intrapatient comparisons. **D)** Representation of the frequency of "CTC-clusters vs single CTCs" pairs with $q<0.01$ and fold change >2 for randomly generated metagenes of the same size as desmosomes (top) and adherence junctions (bottom). Actual number of "CTC-clusters vs single CTCs" pairs with $q<0.01$ and fold change >2 for desmosomes (top) and adherence junctions (bottom) metagenes is shown as a red line. **E)** Representative images of a single CTC and a CTC-cluster captured on the $^{HB}$CTC-Chip from a breast cancer patient and stained with wide-spectrum cytokeratin (CK, red), the desmosome marker desmoplakin (green, top), the adherence junctions marker E-cadherin (green, bottom) and DAPI (nuclei, blue). Related to Figure 6.

**Figure S7. A)** Immunoblot showing the expression levels of plakoglobin and β-Actin (loading control) in lysates from a panel of non-transformed mammary epithelial cells (HMEC, MCF10A) and breast cancer cell lines (LM2, BT474, MCF7, T47D, BT549, BT20, ZR-75-1) expressing control (CTRL) or plakoglobin shRNAs. **B)** Representative brightfield pictures of normal breast cells (HMECs) and breast cancer cells (T47D) grown in monolayer and expressing CTRL or plakoglobin shRNAs. **C)** Representative pictures of LM2-GFP-Luciferase (LM2) and BT474-GFP-Luciferase (BT474) cells expressing CTRL or plakoglobin shRNAs and prepared as single cells (SC) or as clusters (CL) prior to injection into the tail vein of immunodeficient mice. $2x10^5$ LM2 and $4x10^5$ BT474 cells were injected as SC or CL per mouse. **D)** Immunoblot showing the expression levels of plakoglobin and β-Actin (loading control) in lysates from LM2 xenografts expressing CTRL or plakoglobin shRNAs for 30 days. Related to Figure 7.

## EXTENDED EXPERIMENTAL PROCEDURES

### *CTC capture and identification*

Cells captured on the $^{HB}$CTC-Chip were fixed with 4% paraformaldehyde and washed with PBS. Fixed cells were then permeabilized with 1% NP40 in PBS, blocked with 3% goat serum/2% BSA, and immunostained with antibodies against wide spectrum cytokeratin (Abcam), prostate specific antigen (DAKO), prostate-specific membrane antigen (obtained from N. Bander), CD45 (Abcam), plakoglobin (Sigma Aldrich) and DAPI. Alternatively, GFP- or mCherry-expressing cells captured on chip were washed with PBS and imaged directly. Stain-positive cells were detected using the BioView Ltd. automated imaging system (Billerica, MA). High-resolution images were obtained with an upright fluorescence microscope (Eclipse 90i, Nikon, Melville, NY).

$^{neg}$CTC-iChips were designed and fabricated as previously described (Ozkumur et al., 2013). Before processing, whole blood samples were exposed to biotinylated antibodies against CD45 (R&D Systems) and CD66b (AbD Serotec, biotinylated in house) and then incubated with Dynabeads® MyOne™ Streptavidin T1 (Invitrogen) to achieve magnetic labeling and depletion of white blood cells (Ozkumur et al., 2013). The CTC-enriched product was stained in solution with Alexa488-conjugated antibodies against EpCAM (Cell Signaling Technology), Cadherin 11 (R&D Systems) and HER2 (Biolegend) to identify CTCs, and TexasRed-conjugated antibodies against CD45 (BD Biosciences), CD14 (BD Biosciences) and CD16 (BD Biosciences) to identify contaminating white blood cells.

### *Assessment of metastasis-free survival and overall survival*

Kaplan-Meier survival curves based on clinical data from patients at Massachusetts General Hospital were generated with XLStat software (Addinsoft). For “plakoglobin high” vs “plakoglobin low” distant metastasis-free survival in breast cancer patients (as well as for the other CTC-clusters-associated genes) we identified publically available human primary breast cancer gene expression datasets and samples within them having the following characteristics: a) distant-metastasis-free survival information was available, b) there was no evidence of neo-adjuvant treatment, c) the platform used to measure gene expression measured at least 10,000

transcripts, d) if there were multiple samples for a patient, only one was used, e) there were at least 40 samples in the dataset satisfying the preceding criteria. The following datasets were used (Bos et al., 2009; Chanrion et al., 2008; Chin et al., 2006; Desmedt et al., 2007; Li et al., 2010; Loi et al., 2008; Ma et al., 2004; Minn et al., 2007; Minn et al., 2005; Schmidt et al., 2008; Sotiriou et al., 2006; van 't Veer et al., 2002; van de Vijver et al., 2002; Wang et al., 2005). For each dataset, we identified all probes or probesets for plakoglobin and used the one with greatest standard deviation across the samples of the dataset. For each dataset we characterized a sample as "high plakoglobin" if its plakoglobin expression was in the top third of plakoglobin expression for that dataset and as "low plakoglobin" otherwise. We then created a Kaplan-Meier plot and calculated a logrank two-sided p-value using the distant-metastasis-free survival information for the samples from all the datasets and the "high plakoglobin" versus "low plakoglobin" classification.

***Single cell micromanipulation***

The CTC-enriched product was collected in a 35mm petri dish and viewed using a Nikon Eclipse Ti inverted fluorescent microscope. Single CTCs and CTC-clusters were identified based on intact cellular morphology, Alexa488-positive staining and lack of TexasRed staining. Target cells were individually micromanipulated with a 10 μm transfer tip on an Eppendorf TransferMan® NK 2 micromanipulator and ejected into PCR tubes containing RNA protective lysis buffer (10X PCR Buffer II, 25mM MgCl2, 10% NP40, 0.1 M DTT, SUPERase-In, Rnase Inhibitor, 0.5 uM UP1 Primer, 10mM dNTP and Nuclease-free water) and immediately flash frozen in liquid nitrogen.

***Single Cell RNA Amplification and Sequencing***

RNA samples extracted from CTCs were thawed on ice and incubated at 70°C for 90 seconds. To generate cDNA, samples were treated with reverse transcription master mix (0.05 uL RNase inhibitor, 0.07uL T4 gene 32 protein, and 0.33uL SuperScript III Reverse Transcriptase per 1X volume) and incubated on thermocycler at 50°C for 30 minutes and 70°C for 15 minutes. To remove free primers, 1.0uL of EXOSAP mix was added to each sample, which was incubated at 37°C for 30 minutes and inactivated at 80°C for 25 minutes. Next, a 3'-poly-A tail was added to the cDNA in each sample by incubating in master mix (0.6uL 10X PCR Buffer II, 0.36uL 25mM

$MgCl_2$, 0.18uL 100mM dATP, 0.3uL Terminal Transferase, 0.3uL RNase H, and 4.26uL $H_2O$ per 1X volume) at 37°C for 15 minutes and inactivated at 70°C for 10 minutes. A second strand cDNA was synthesized by dividing each sample into 4 and incubating in master mix (2.2uL 10X High Fidelity PCR Buffer, 1.76uL 2.5mM each dNTP, 0.066uL UP2 Primer at 100uM, 0.88uL 50mM $MgSO_4$, 0.44uL Platinum Taq DNA Polymerase, and 13.654uL $H_2O$ per 1X volume) at 95°C for 3 minutes, 50°C for 2 minutes, and 72°C for 10 minutes. PCR amplification (95°C for 3 minutes, 20 cycles of 95°C for 30 seconds, 67°C for 1 minute, and 72°C for 6 minutes 6 seconds) was performed with master mix (4.1uL 10X High Fidelity PCR Buffer, 1.64uL 50mM $MgSO_4$, 4.1uL 2.5mM each dNTP, 0.82uL AUP1 Primer at 100uM, 0.82uL AUP2 Primer at 100uM, 0.82uL Platinum Taq DNA Polymerase, and 6.7uL $H_2O$ per 1X volume). The 4 reactions of each sample were pooled and purified using the QIAGEN PCR Purification Kit (Cat. No 28106) and eluted in 50uL EB buffer. Samples were selected by testing for genes Gapdh, ActB, Ptprc (CD45), Krt8, Krt18 and Krt19 using qPCR. Each sample was again divided in 4 and a second round of PCR amplification (9 cycles of 98°C for 3 minutes, 67°C for 1 minute, and 72°C for 6 minutes 6 seconds) was performed with master mix (9uL 10X High Fidelity PCR Buffer, 3.6uL 50mM $MgSO_4$, 13.5uL 2.5mM each dNTP, 0.9uL AUP1 Primer at 100uM, 0.9uL AUP2 Primer at 100uM, 1.8uL Platinum Taq DNA Polymerase, and 59.1uL $H_2O$ per 1X volume). Samples were pooled and purified using Agencourt AMPure XP beads and eluted in 40uL 1X low TE buffer.

***Sequencing Library Construction***

To shear the DNA using the Covaris S2 System, 1X low TE buffer and 1.2uL shear buffer were added to each sample. Conditions of the shearing program include: 6 cycles, 5°C bath temperature, 15°C bath temperature limit, 10% duty cycle, intensity of 5, 100 cycles/burst, and 60 seconds. Then, samples were end-polished at room temperature for 30 minutes with a master mix (40uL 5X Reaction Buffer, 8uL 10mM dNTP, 8uL End Polish Enzyme1, 10uL End Polish Enzyme2, and 14uL $H_2O$ per 1X volume). DNA fragments larger than 500bp were removed with 0.5X volumes of Agencourt AMPure XP beads. Supernatant was transferred to separate tubes. To size-select 200-500bp DNA products, 0.3X volumes of beads were added and samples were washed twice with 70% EtOH. The products were eluted in 36uL low TE buffer. A dA-tail was added to each size-selected DNA by treating with master mix (10uL 5X Reaction Buffer, 1uL

10mM dATP, and 5uL A-Tailing Enzyme I per 1X volume) and incubated at 68°C for 30 minutes and cooled to room temperature. To label and distinguish each DNA sample for sequencing, barcode adaptors (5500 SOLiD 4464405) were ligated to DNA using the 5500 SOLiD Fragment Library Enzyme Module (4464413). Following barcoding, samples were purified twice using the Agencourt AMPure XP beads and eluted in 22uL low TE buffer. Following a round of PCR Amplification (95°C for 5 minutes, 12 cycles of 95°C for 15 seconds, 62°C for 15 seconds, and 70°C for 1 minute, and 70°C for 5 minutes), the libraries were purified with AMPure XP beads. Finally, to quantify the amount of ligated DNA, SOLiD Library TaqMan Quantitation Kit was used to perform qPCR. Completed barcoded libraries were then subjected to emulsion PCR with template beads preparation and sequenced on the ABI 5500XL.

***Analysis of RNA Sequencing data***

Clustering: the minimum of 1 and the smallest positive value of the rpm matrix was added to the rpm matrix to eliminate zeros. The result was then log transformed and median polished. The rows (corresponding to genes) with the top 2000 standard deviations were retained and the rest of the rows discarded. The result was clustered using agglomerative hierarchical clustering with average linkage with distance metric equal to 1 minus the Pearson correlation coefficient.

Supervised differential gene expression: samples that showed high expression of contaminant WBC markers and no expression of CTC markers at the RNA level were excluded from the analysis. For each pair of single CTCs sample and CTC-cluster sample from the same patient, we calculated a FDR q-value and a normalized fold-change using the DEGexp function of version 1.10.0 of the Bioconductor DEGseq package (Wang et al., 2010) with method set to ‘MARS’ and q-values calculated using Benjamini-Hochberg. For each pair and direction (e.g., up in CTC-clusters vs. single CTCs) a gene was considered a hit if its q-value was less than 0.01 and its fold-change was greater than 2. Then, for each direction, we considered the genes that were hits for 70% or more of the pairs. The desmosome (resp. adherence junction) metagene was defined to be the mean over the desmosome (resp. adherence junction) marker genes of the normalized log2 fold change between the CTC-clusters and the single CTCs as determined by DEGseq.

***In Vivo Flow Cytometry***

DiD-labeled LM2 single or clustered cells were adoptively transferred intravenously and detected in the peripheral circulation (Novak et al., 2004). Of note, single and clustered LM2 cells were injected separately in different animals to avoid signal misinterpretation. DiD was excited by a 635 nm laser and detected with a 695 ± 27.5 nm bandpass filter using a photomultiplier tube. Circulation kinetics for LM2-SCs and LM2-CLs were quantified using MATLAB (Mathworks).

***Immunohistochemistry***

Formalin-fixed and paraffin embedded mouse xenografts primary tumors, lung metastases, as well as human primary tumors and matched metastatic lesions were sectioned and stained overnight at 4°C with antibodies against cleaved caspase 3 (Cell Signaling Technology), GFP (Cell signaling Technology), mCherry (Abcam), plakoglobin (Sigma Aldrich) and CD31 (Abcam). GFP/mCherry and Plakoglobin/CD31 double-stainings were performed with EnVision™ G/2 Doublestain System (Dako). All specimens were counterstained with Hematoxylin. Images of the whole tissue were taken with ScanScope (Aperio).

***Cell culture and reagents***

HMEC, MCF10A, BT474, MCF7, T47D, 4T1, BT549, BT20 and ZR-75-1 cells were purchased from the American Type Culture Collection (ATCC) and propagated according to the manufacturer's instructions. MDA-MB-231 LM2 cells were obtained from J. Massague (MSKCC, New York, NY, USA) and propagated in DMEM (Life Technologies) supplemented with 10% fetal bovine serum (Life Technologies). To generate BT474, 4T1 or LM2 single cells or clusters for tail vein injections, cells growing in monolayer at 80% confluence were incubated with trypsin (Life Technologies) for one minute to generate floating clusters. Clusters were then distributed equally in two separate dishes. In one of the two dishes, clusters were mechanically dissociated by pipetting to generate a single cell suspension.

Cell-to-cell adhesion assay was performed with the Vybrant® Cell-to-Cell Adhesion Assay Kit (Invitrogen) according to the manufacturer's instructions.

The plasmid expressing GFP-Luciferase was obtained from C. Ponzetto (University of Torino, Italy). The plasmid expressing mCherry was purchased from Addgene. Plakoglobin TRC

shRNAs were purchased from Thermo Scientific. Lentiviral packaging vectors (Addgene) were used to transfect 293T cells (ATCC) and produce lentiviral particles. Infections of target cells lines was performed overnight at a MOI=10 in growth medium containing 8 μg/ml polybrene (Thermo Scientific).

## SUPPLEMENTAL REFERENCES


Bos, P.D., Zhang, X.H., Nadal, C., Shu, W., Gomis, R.R., Nguyen, D.X., Minn, A.J., van de Vijver, M.J., Gerald, W.L., Foekens, J.A., *et al.* (2009). Genes that mediate breast cancer metastasis to the brain. Nature *459*, 1005-1009.

Chanrion, M., Negre, V., Fontaine, H., Salvetat, N., Bibeau, F., Mac Grogan, G., Mauriac, L., Katsaros, D., Molina, F., Theillet, C., *et al.* (2008). A gene expression signature that can predict the recurrence of tamoxifen-treated primary breast cancer. Clinical cancer research : an official journal of the American Association for Cancer Research *14*, 1744-1752.

Chin, K., DeVries, S., Fridlyand, J., Spellman, P.T., Roydasgupta, R., Kuo, W.L., Lapuk, A., Neve, R.M., Qian, Z., Ryder, T., *et al.* (2006). Genomic and transcriptional aberrations linked to breast cancer pathophysiologies. Cancer cell *10*, 529-541.

Desmedt, C., Piette, F., Loi, S., Wang, Y., Lallemand, F., Haibe-Kains, B., Viale, G., Delorenzi, M., Zhang, Y., d'Assignies, M.S., *et al.* (2007). Strong time dependence of the 76-gene prognostic signature for node-negative breast cancer patients in the TRANSBIG multicenter independent validation series. Clinical cancer research : an official journal of the American Association for Cancer Research *13*, 3207-3214.

Li, Y., Zou, L., Li, Q., Haibe-Kains, B., Tian, R., Li, Y., Desmedt, C., Sotiriou, C., Szallasi, Z., Iglehart, J.D., *et al.* (2010). Amplification of LAPTM4B and YWHAZ contributes to chemotherapy resistance and recurrence of breast cancer. Nature medicine *16*, 214-218.

Loi, S., Haibe-Kains, B., Desmedt, C., Wirapati, P., Lallemand, F., Tutt, A.M., Gillet, C., Ellis, P., Ryder, K., Reid, J.F., *et al.* (2008). Predicting prognosis using molecular profiling in estrogen receptor-positive breast cancer treated with tamoxifen. BMC genomics *9*, 239.

Ma, X.J., Wang, Z., Ryan, P.D., Isakoff, S.J., Barmettler, A., Fuller, A., Muir, B., Mohapatra, G., Salunga, R., Tuggle, J.T., *et al.* (2004). A two-gene expression ratio predicts clinical outcome in breast cancer patients treated with tamoxifen. Cancer cell *5*, 607-616.

Minn, A.J., Gupta, G.P., Padua, D., Bos, P., Nguyen, D.X., Nuyten, D., Kreike, B., Zhang, Y., Wang, Y., Ishwaran, H., *et al.* (2007). Lung metastasis genes couple breast tumor size and metastatic spread. Proceedings of the National Academy of Sciences of the United States of America *104*, 6740-6745.

Minn, A.J., Gupta, G.P., Siegel, P.M., Bos, P.D., Shu, W., Giri, D.D., Viale, A., Olshen, A.B., Gerald, W.L., and Massague, J. (2005). Genes that mediate breast cancer metastasis to lung. Nature *436*, 518-524.

Novak, J., Georgakoudi, I., Wei, X., Prossin, A., and Lin, C.P. (2004). In vivo flow cytometer for real-time detection and quantification of circulating cells. Optics letters *29*, 77-79.

Ozkumur, E., Shah, A.M., Ciciliano, J.C., Emmink, B.L., Miyamoto, D.T., Brachtel, E., Yu, M., Chen, P.I., Morgan, B., Trautwein, J., *et al.* (2013). Inertial focusing for tumor antigen-

dependent and -independent sorting of rare circulating tumor cells. Science translational medicine *5*, 179ra147.
Schmidt, M., Bohm, D., von Torne, C., Steiner, E., Puhl, A., Pilch, H., Lehr, H.A., Hengstler, J.G., Kolbl, H., and Gehrmann, M. (2008). The humoral immune system has a key prognostic impact in node-negative breast cancer. Cancer research *68*, 5405-5413.
Sotiriou, C., Wirapati, P., Loi, S., Harris, A., Fox, S., Smeds, J., Nordgren, H., Farmer, P., Praz, V., Haibe-Kains, B., *et al.* (2006). Gene expression profiling in breast cancer: understanding the molecular basis of histologic grade to improve prognosis. Journal of the National Cancer Institute *98*, 262-272.
van 't Veer, L.J., Dai, H., van de Vijver, M.J., He, Y.D., Hart, A.A., Mao, M., Peterse, H.L., van der Kooy, K., Marton, M.J., Witteveen, A.T., *et al.* (2002). Gene expression profiling predicts clinical outcome of breast cancer. Nature *415*, 530-536.
van de Vijver, M.J., He, Y.D., van't Veer, L.J., Dai, H., Hart, A.A., Voskuil, D.W., Schreiber, G.J., Peterse, J.L., Roberts, C., Marton, M.J., *et al.* (2002). A gene-expression signature as a predictor of survival in breast cancer. The New England journal of medicine *347*, 1999-2009.
Wang, L., Feng, Z., Wang, X., Wang, X., and Zhang, X. (2010). DEGseq: an R package for identifying differentially expressed genes from RNA-seq data. Bioinformatics *26*, 136-138.
Wang, Y., Klijn, J.G., Zhang, Y., Sieuwerts, A.M., Look, M.P., Yang, F., Talantov, D., Timmermans, M., Meijer-van Gelder, M.E., Yu, J., *et al.* (2005). Gene-expression profiles to predict distant metastasis of lymph-node-negative primary breast cancer. Lancet *365*, 671-679.

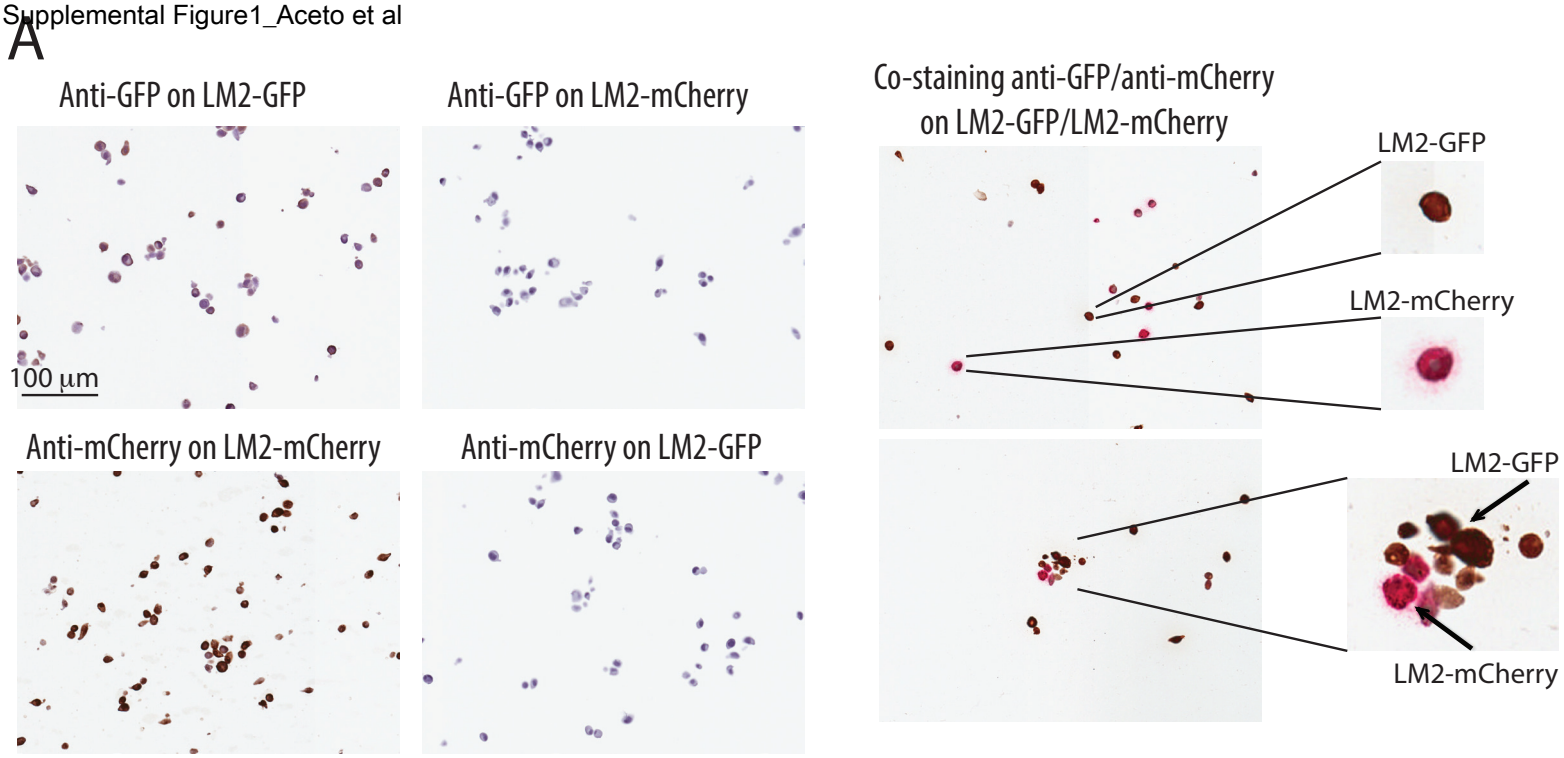


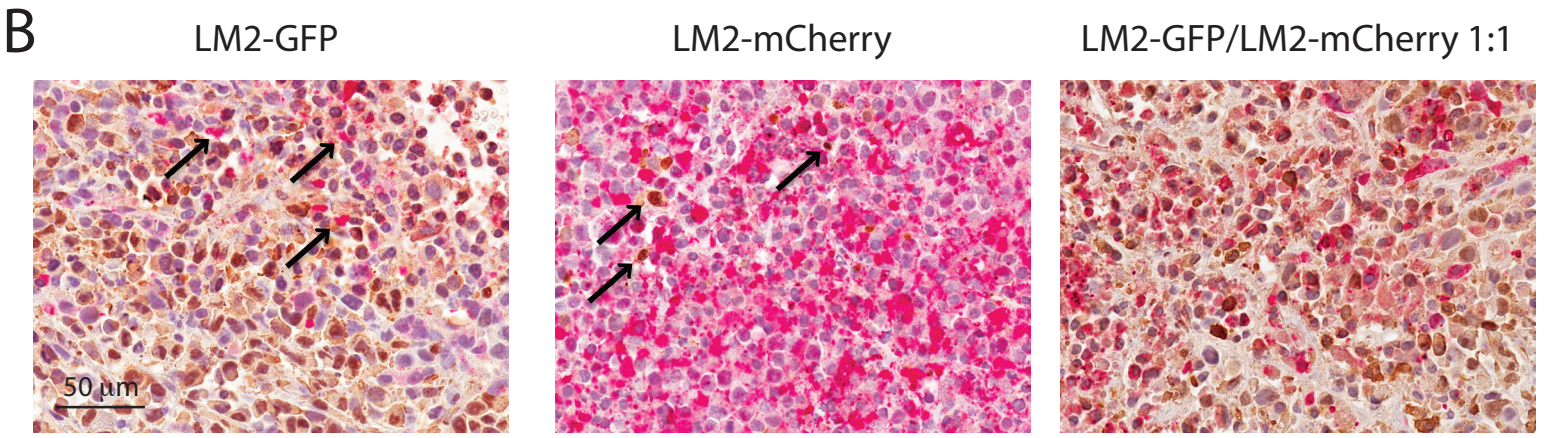


FIGURE S1 Aceto et al.

A

LM2-GFP/LM2-mCherry 1:1 MODEL

| | HB CTC-chip |
|---|---|
| One color (single CTCs) | 2421 ± 240.5 |
| Multicolor (single CTCs) | 0 ± 0 |
| One color (CTC-clusters) | 5.6 ± 1.4 |
| Multicolor (CTC-clusters) | 60 ± 7.2 |

| | Lung foci |
|---|---|
| One color | 151.8 ± 16.8 |
| Multicolor | 171.2 ± 30.4 |

LM2-GFP (right) and LM2-mCherry (left) MODEL

| | HB CTC-chip |
|---|---|
| One color (single CTCs) | 3581.4 ± 413.4 |
| Multicolor (single CTCs) | 0 ± 0 |
| One color (CTC-clusters) | 119 ± 10.3 |
| Multicolor (CTC-clusters) | 4.8 ± 2.9 |

| | Lung foci |
|---|---|
| One color | 329.8 ± 35.5 |
| Multicolor | 29.4 ± 7.9 |

B

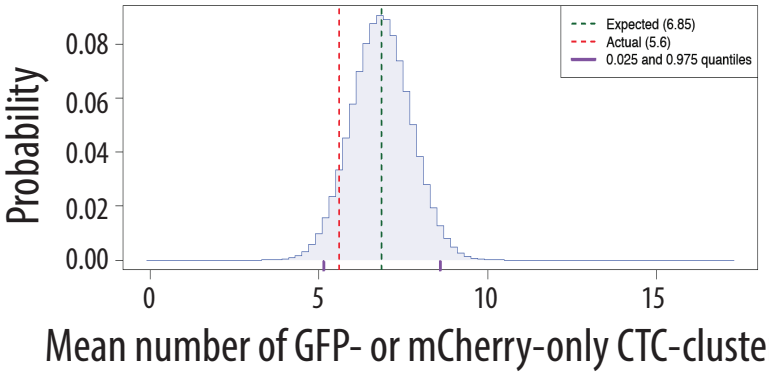


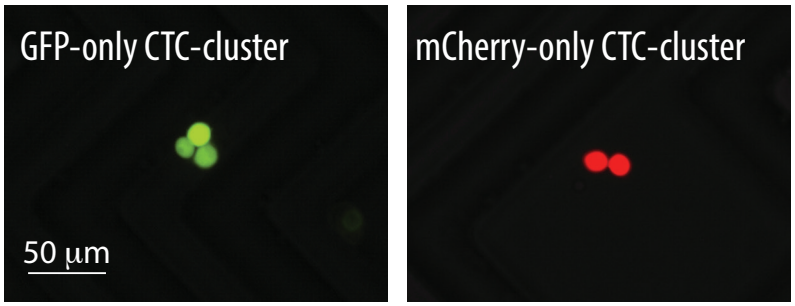


C

4T1-GFP/4T1-mCherry 1:1 MODEL

| | HB CTC-chip |
|---|---|
| One color (single CTCs) | 1679.7 ± 266.2 |
| Multicolor (single CTCs) | 0 ± 0 |
| One color (CTC-clusters) | 10.5 ± 3.6 |
| Multicolor (CTC-clusters) | 93.5 ± 33.1 |

| | Lung foci |
|---|---|
| One color | 223 ± 20.7 |
| Multicolor | 202.2 ± 17.9 |

4T1-GFP (right) and 4T1-mCherry (left) MODEL

| | HB CTC-chip |
|---|---|
| One color (single CTCs) | 3384.7 ± 306.3 |
| Multicolor (single CTCs) | 0 ± 0 |
| One color (CTC-clusters) | 249.7 ± 56.7 |
| Multicolor (CTC-clusters) | 37.7 ± 19.6 |

| | Lung foci |
|---|---|
| One color | 498.2 ± 71.4 |
| Multicolor | 82 ± 24.6 |

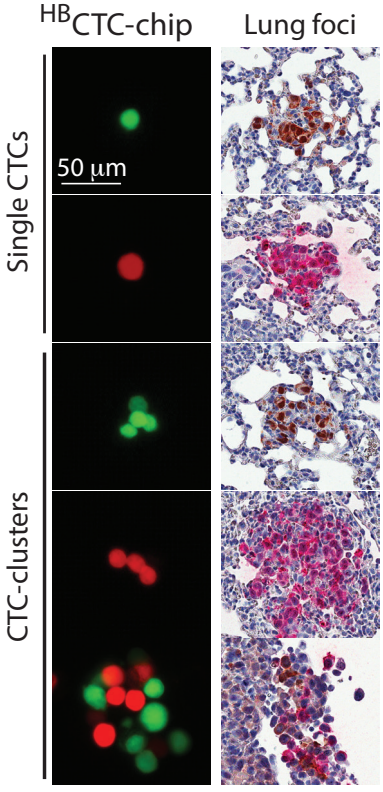


D

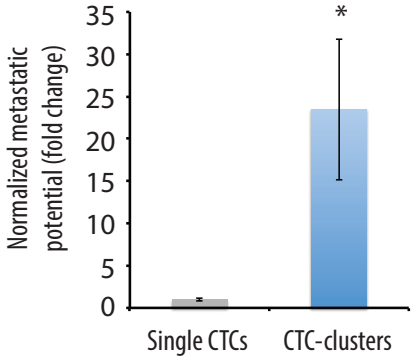


FIGURE S2 Aceto et al.

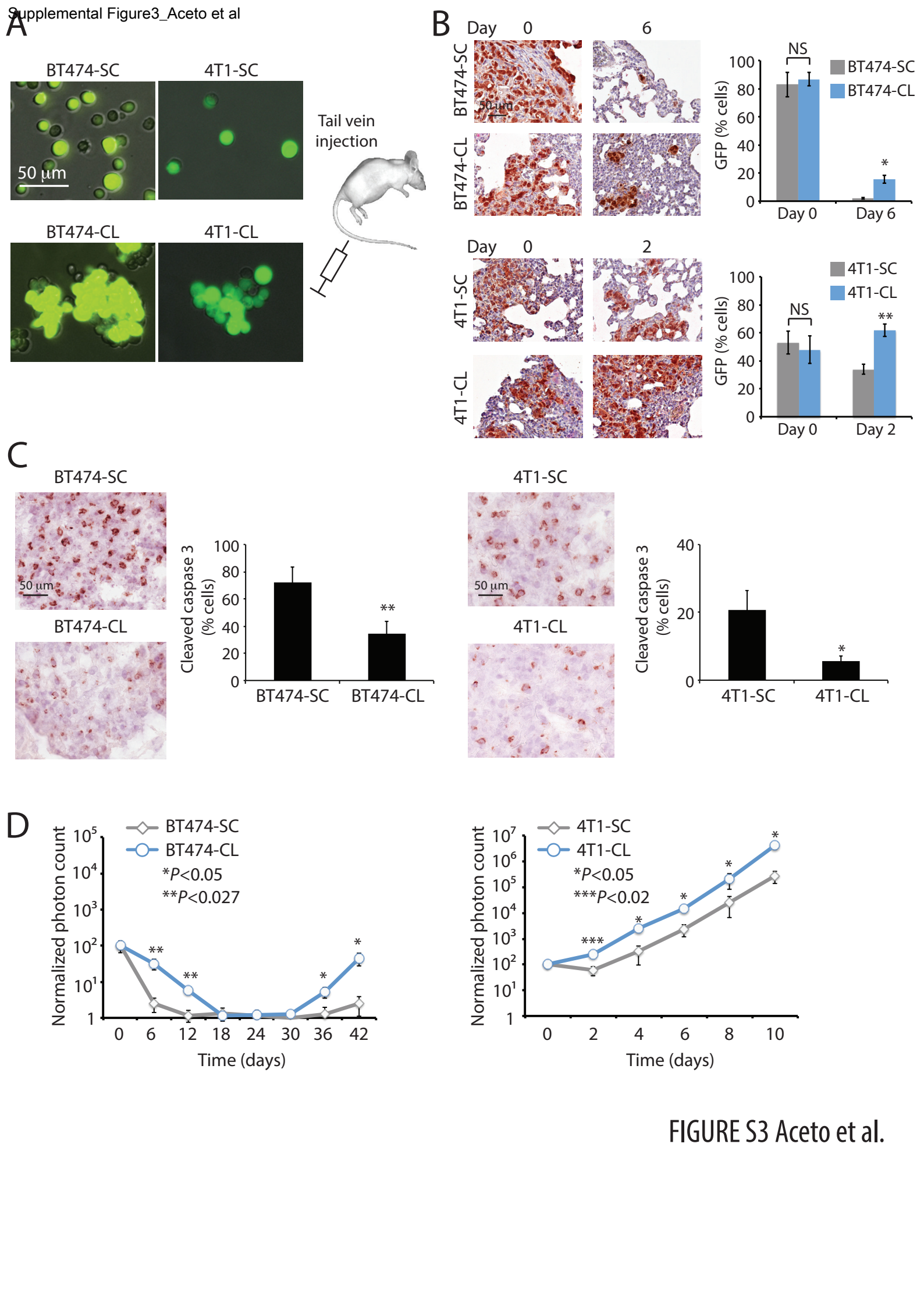


FIGURE S3 Aceto et al.

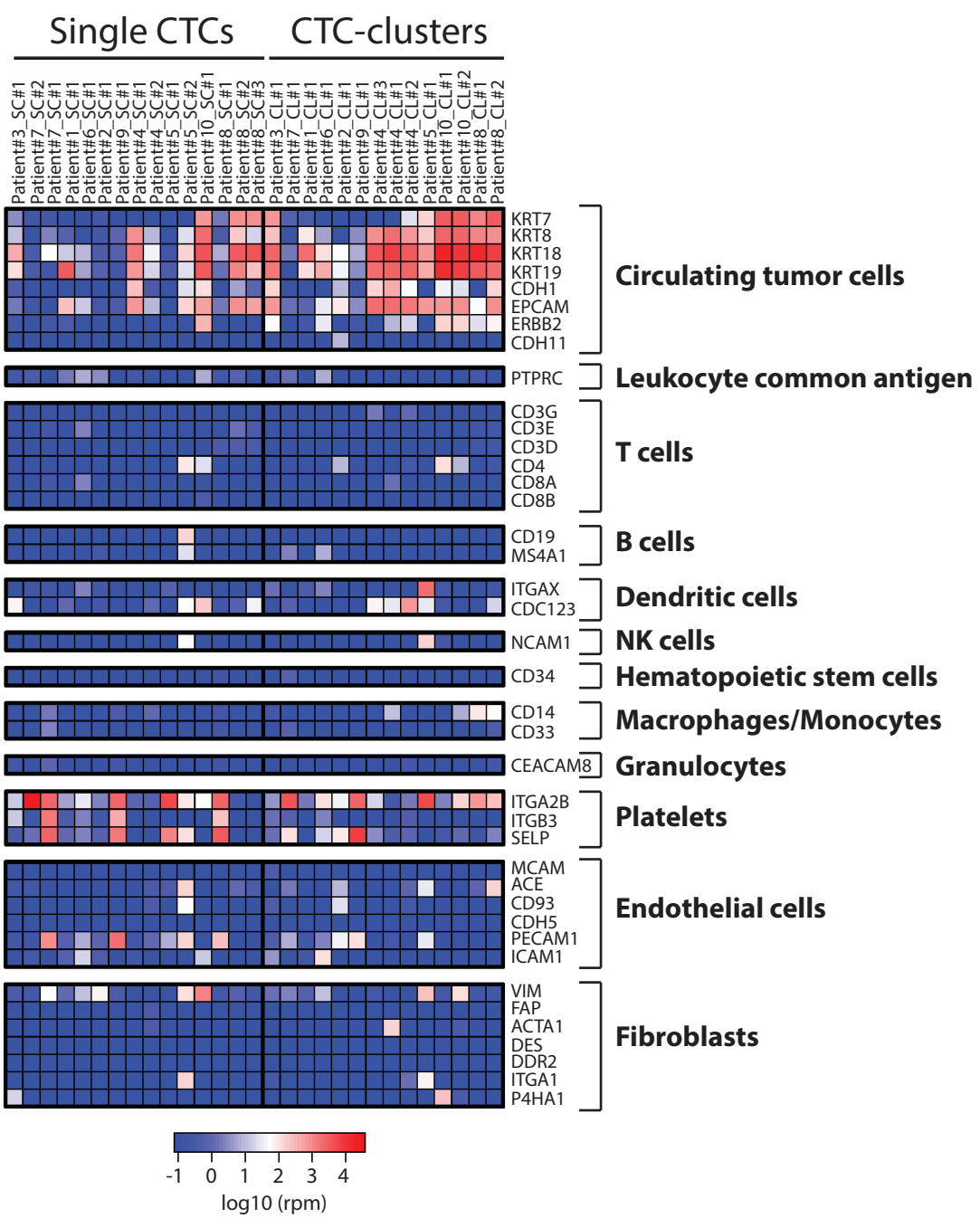


FIGURE S4 Aceto et al.

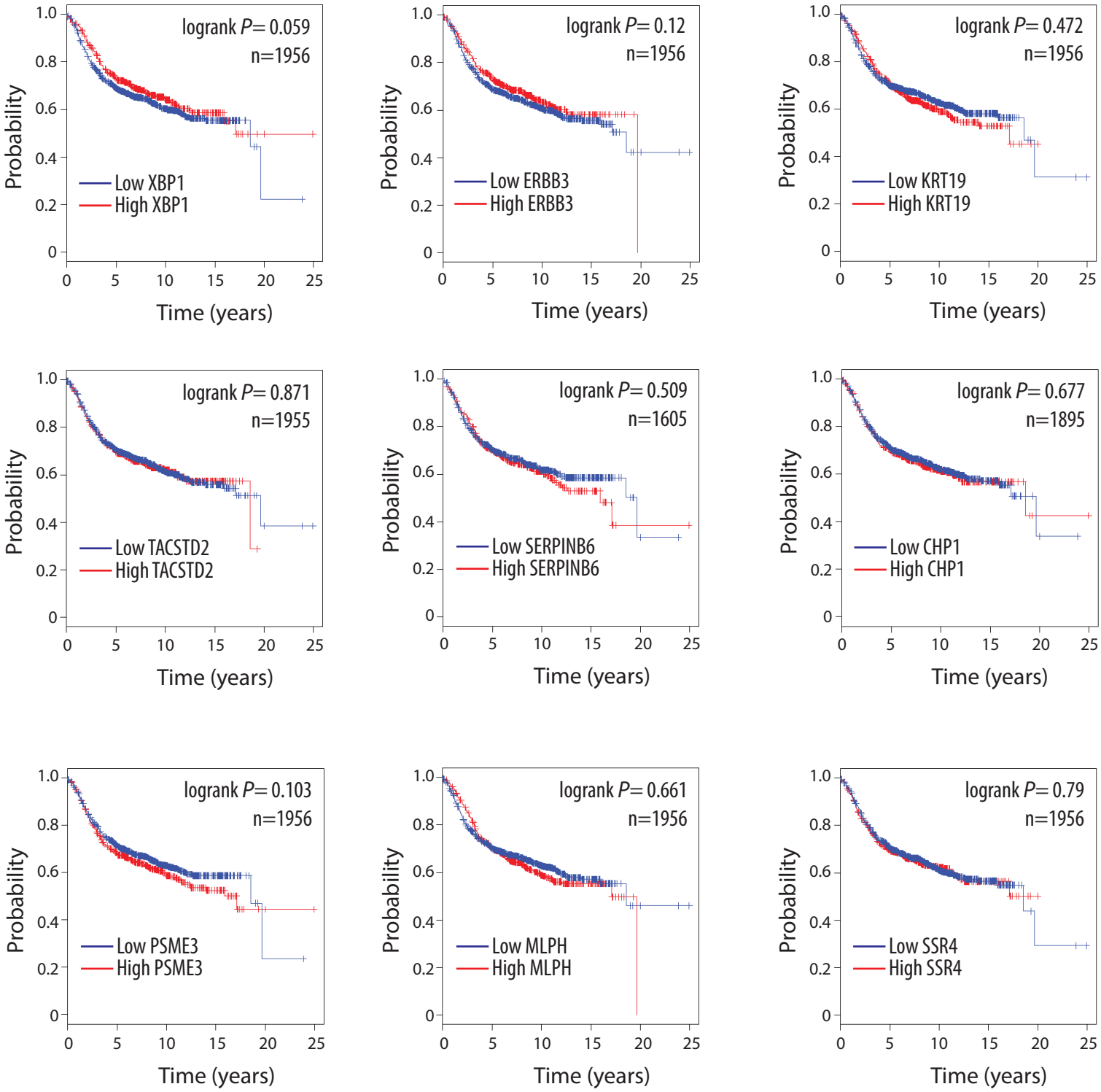


FIGURE S5 Aceto et al.

Supplemental Figure6_Aceto et al

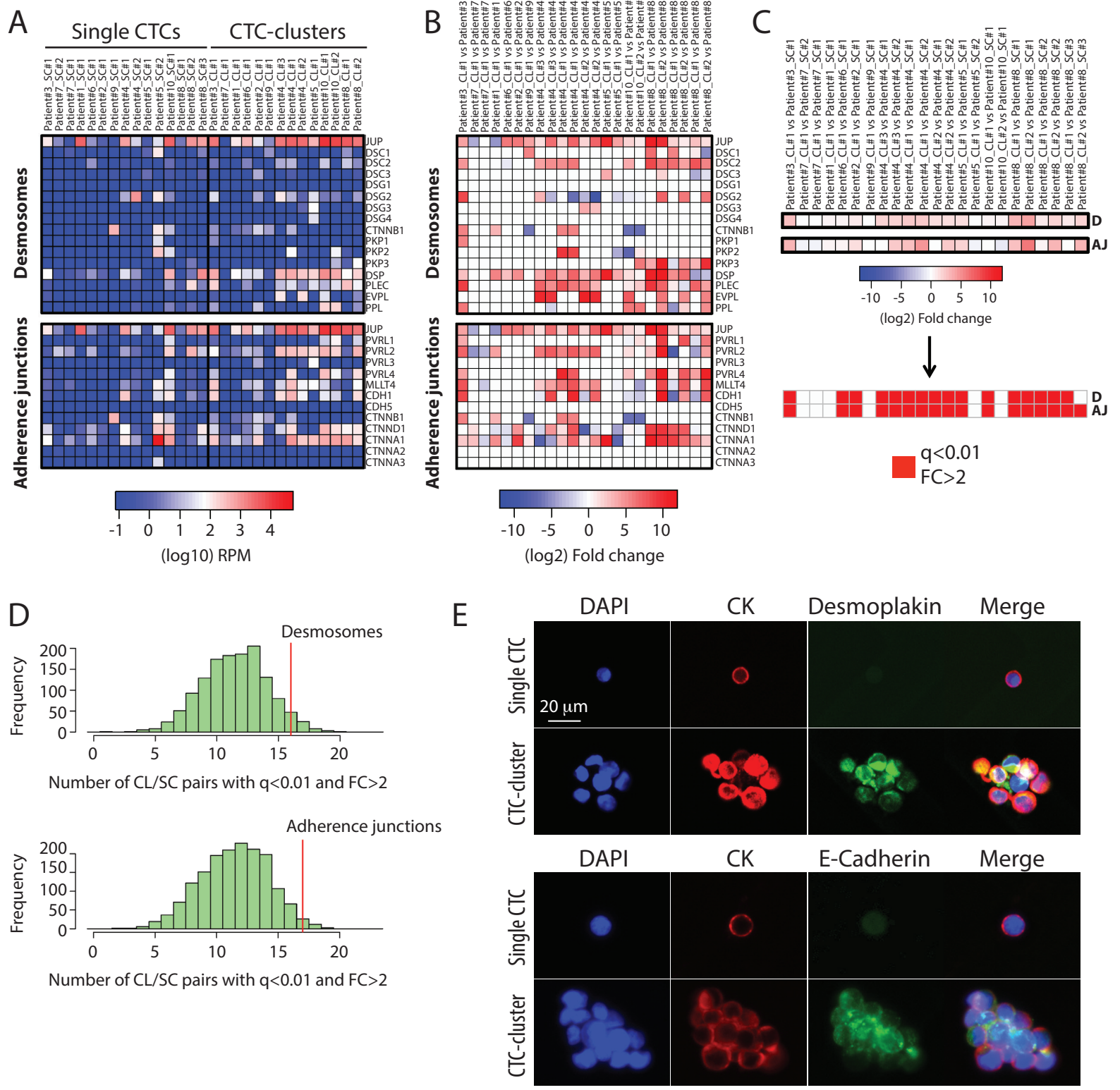








FIGURE S6 Aceto et al.

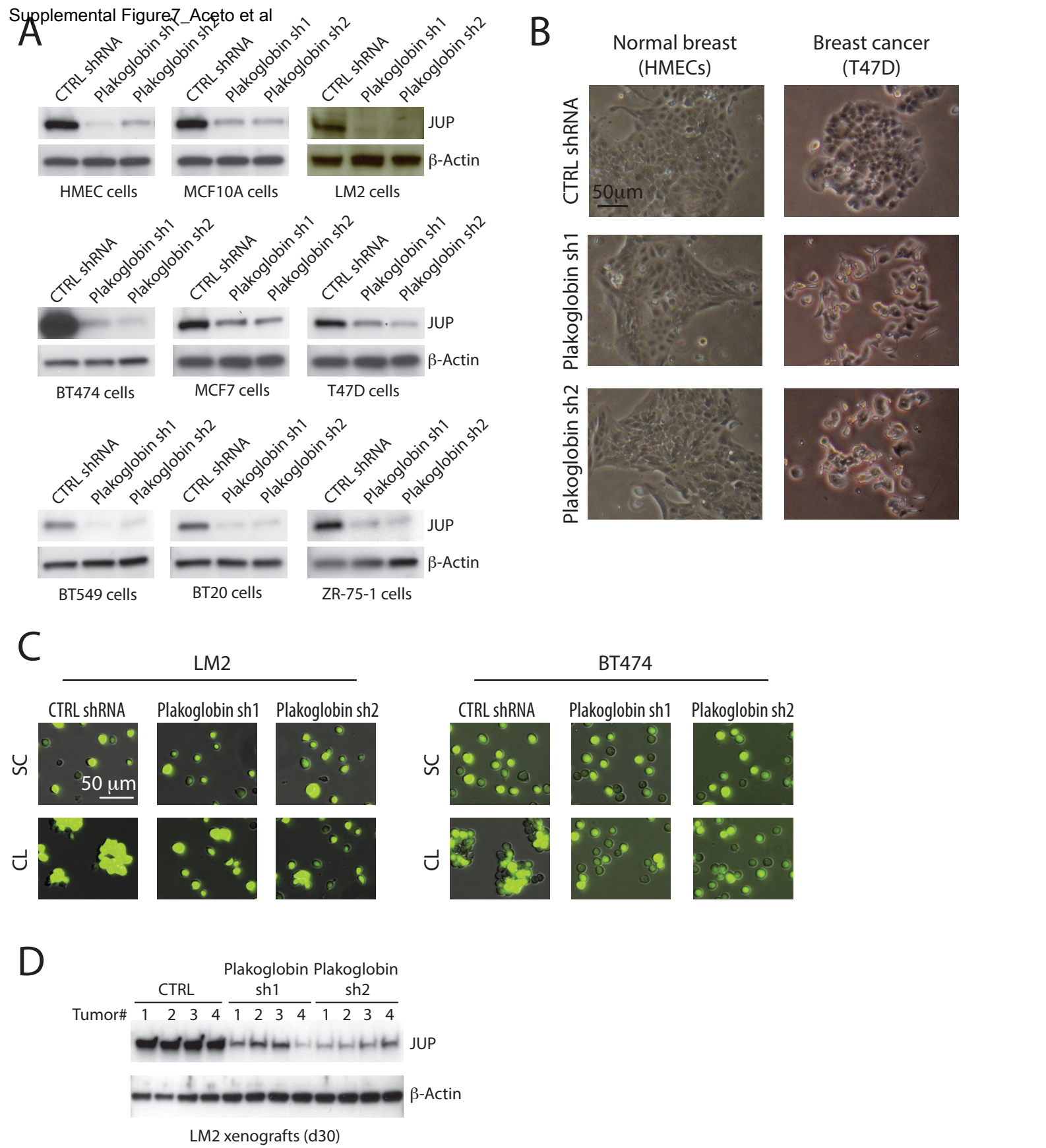


FIGURE S7 Aceto et al.